

Single Molecule Force Spectroscopy on Polyelectrolytes: Effect of Spacer on Adhesion Force and Linear Charge Density on Rigidity

Shuxun Cui, Chuanjun Liu, Zhiqiang Wang, and Xi Zhang*

Key Lab of Organic Optoelectronics and Molecular Engineering, Department of Chemistry, Tsinghua University, Beijing 100084, P. R. China, and Key Lab for Supramolecular Structure and Materials, College of Chemistry, Jilin University, Changchun 130023, P. R. China

Satu Strandman and Heikki Tenhu

Lab of Polymer Chemistry, Department of Chemistry, University of Helsinki, Finland

Received September 18, 2003; Revised Manuscript Received November 25, 2003

ABSTRACT: We have synthesized a new kind of poly(2-acrylamido-2-methylpropanesulfonic acid) with crown ether and studied comparatively the single molecule force spectroscopy of the polymers with and without crown ether, in terms of desorption and elongation. The smooth desorption process enabled us to calculate the loading rate of the stretching process. For the two polymers, desorption forces were loading rate independent and ionic strength insensitive. Interestingly, the desorption forces of the two polymers were undistinguishable in all conditions. These findings demonstrate (1) the polymer chains adopt a trainlike (flat) conformation at the interface with a high adsorption/desorption rate, (2) the spacer, which separates the charged group from the hydrophobic backbone and combines the two properties together, should account for the retained desorption force at high salt concentration, and (3) the 20% less in linear charge density does not affect the desorption force remarkably since hydrophobic interaction dominates the adhesion force. In deionized water, PAMPS-*co*-crown is less rigid than PAMPS since the uncharged side groups separate the charged groups, and thus the repulsion between adjacent charged groups is reduced. As the salt concentration increased, the rigidity of the two polymers both decreased, suggesting that the external salt would screen the charges of the polyelectrolytes. The linear charge density and the ionic strength affect only the rigidity of single polyelectrolyte chain but not the adhesion force, which is another result of the “spacer effect”. This fundamental finding, which reveals the nonelectrostatic origin of the interfacial interaction of polyelectrolytes, sheds new light on the understanding of polyelectrolytes, especially for those containing spacers.

Introduction

Polyelectrolytes, as an important class of functional polymers, have been widely studied over 40 years, and now they are still arousing more and more attention due to their unique properties at interfaces, for example, to precipitate small particles in a variety of processes, including mineral separation, flocculation, retention, or as strength-enhancing additives in paper production. Beyond neutral polymer, polyelectrolyte is a more complicated challenging system for scientists working in both experiment and theory. In the generally accepted Onsager–Manning model,¹ a charged cylindrical polyion and all of its counterions are confined within a “cylindrical cell”. The sum of all charges inside each cylindrical cell is zero. Ignoring the influence of the system's free energy and the differences among polyions, this model is oversimplified. A proper, generalized model is required to cover all the range of polyelectrolytes, demanding abundant single molecule experimental results as basis. However, the direct measurement on the behavior of single polyelectrolyte chain, which is crucial to further understanding of the complicated system, was difficult in the past years.

The emergence of atomic force microscopy (AFM) enabled one not only to detect the surface morphology in the nanometer scale but also to manipulate a single molecule at a surface for the first time.² Recently, single molecule force spectroscopy (SMFS), based on AFM, has

become a versatile platform for studying intermolecular and intramolecular interactions with extremely high force sensitivity.^{3,4} Using SMFS, a number of interesting topics, such as protein unfolding,^{5,6} DNA unzipping,^{7,8} force-induced conformational transition,⁹ host–guest interaction,¹⁰ single chain elasticity,^{11–13} and single chain desorption from substrate,^{14–16} have been investigated. As a recent progress, Seitz et al. reported the single chain behavior of a polyelectrolyte lacking a spacer, polyvinylamine, on the addition of external salt.¹⁷

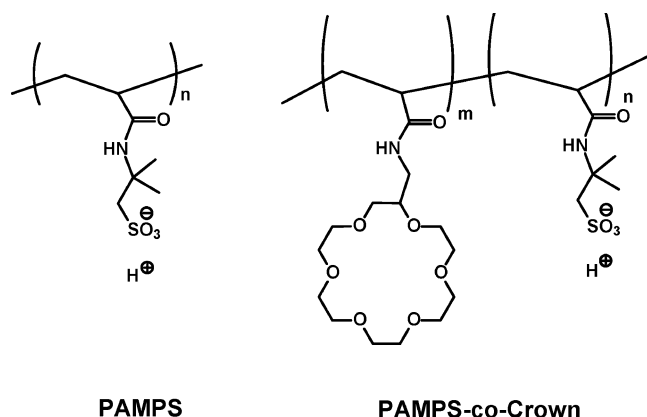
In this paper, we have synthesized a new kind of poly(2-acrylamido-2-methylpropanesulfonic acid) with crown ether and studied comparatively the single molecule force spectroscopy of the polymers with and without crown ether. The research is conducted in terms of desorption and elongation. We discover the influences of the spacer and the linear charge density on the adhesion force and the rigidity of single polyelectrolyte chain. These results are significant for further understanding as well as for rational design of polyelectrolytes.

Experiment

Materials. The structures of the polymers poly(2-acrylamido-2-methylpropanesulfonic acid) (PAMPS) and its random copolymer containing 18-crown-6 (PAMPS-*co*-crown) are shown in Scheme 1. Potassium chloride and other reagents are of analytical reagent grade. Deionized water (DI water, > 18 MΩ cm, pH 5.7) is used when water is involved.

Polymers Synthesis and Characterization. 2-Amino-methyl-(18-crown-6) (Aldrich, 95%), triethylamine (Et₃N),

* Corresponding author. E-mail: xi@jlu.edu.cn.

Scheme 1. Primary Structures of PAMPS and PAMPS-co-crown

acrylamido-2-methyl-2-propanesulfonic acid (AMPS), and *tert*-butyl alcohol (all from Merck) were used as received. Acryloyl chloride (Merck) was dried with molecular sieves and distilled at normal pressure. 1,4-Dioxane (from Riedel de-Haën) was dried with molecular sieves and vacuum-distilled. α, α' -Azobisisobutyronitrile (AIBN, Fluka) was recrystallized in methanol.

The ^1H and ^{13}C NMR spectra of the polymers were measured on 200 MHz Varian Gemini 2000 NMR spectrometer (operating at 200 MHz for ^1H and at 50.3 MHz for ^{13}C). The chemical shifts are presented in part per million (ppm) downfield from internal TMS standard in CDCl_3 or using either D_2O or the crown ether main peak at 71 ppm as a reference. The size-exclusion chromatography (SEC) analyses were performed on a Waters instrument with 7.8×300 mm Ultrahydrogel capillary column and a Waters 2410 RI detector. 0.1 M NaNO_3 aqueous solution with 3 vol % of acetonitrile was used as an eluent at a flow rate 0.8 mL/min. The calibration was performed against poly(ethylene oxide) or poly(acrylic acid) standards.

Synthesis of the Crown Ether Monomer (Acrylamidomethyl-18-crown-6). 2-Aminomethyl-(18-crown-6) (3.0 g, 10.2 mmol) and Et_3N (0.610 g, 10.3 mmol) were dissolved in 1,4-dioxane (12 mL), and the mixture was cooled to 0 °C. Acryloyl chloride (3.0 g, 33.1 mmol) was dissolved in 1,4-dioxane (7.2 mL) and slowly added to the cooled solution. The temperature was slowly raised to room temperature, and the mixture was stirred for 6 h. The precipitate ($\text{Et}_3\text{N} \cdot \text{HCl}$) was removed by filtration. The excess acryloyl chloride and the solvent were evaporated. The product was a yellow viscous oil, $m = 3.504$ g. This product was used in the following polymerization.

^1H NMR (200 MHz, CDCl_3) δ ppm: 2.32 (1 H, $-\text{CH}-$ 18-crown-6), 2.80 (2 H, $-\text{CH}_2-$ (18-crown-6)), 3.63 (22 H, 18-crown-6), 5.5–6.5 (3 H, vinyl protons). ^{13}C NMR (200 MHz, CDCl_3) δ ppm: 41 (1 C, $-\text{CH}_2-$ (18-crown-6)), 67–76 (12 C, 18-crown-6), 126 (1 C, $-\text{C}_\alpha\text{H}-$), 131 (1 C, $-\text{C}_\beta\text{H}_2-$), 166 (1 C, $>\text{C}=\text{O}$).

Synthesis of the PAMPS-co-crown Copolymer. AMPS (2.98 g, 14.4 mmol) was dissolved in *tert*-butyl alcohol (248 mL). Acrylamidomethyl-18-crown-6 (2.14 g, 6.2 mmol) was dissolved in 10 mL of solvent and added to the solution of AMPS. The initial monomer ratio was 70:30 mol % (AMPS: crown), and the concentration of the monomers was 0.08 M. The temperature was kept at 35 °C, above the melting point of *tert*-butyl alcohol. The solution was deaerated with nitrogen for 2 h, after which the temperature was brought to 65 °C and AIBN (73 mg, 0.44 mmol, 2.2 mol %) was added to the solution.

The nitrogen flow was stopped 15 min after the introduction of the initiator. The reaction time was 19 h. A yellow viscous polymer was dissolved in water, purified by dialysis, and dried in vacuo at room temperature. A yellow film was obtained; $m(\text{polymer}) = 2.39$ g, yield 47%.

The monomer ratio was determined by NMR spectroscopy and titrimetrically, being 80:20 mol % (AMPS:crown). M_n

(SEC, PEO standards) = 47 000 g/mol; PDI = 1.68. A PAMPS-co-crown chain with molecular weight of M_n has a contour length of 51 nm.

^1H NMR (200 MHz, D_2O) δ ppm: 0.83 ($-\text{NH}-$), 1.49 (10 H, $-\text{CH}_3$ and $-\text{C}_\beta\text{H}_2-$), 2.19 (2 H, $-\text{C}_\alpha\text{H}-$), 3.37 (4 H, $-\text{CH}_2\text{SO}_3\text{H}$ and $-\text{CH}_2-$ (18-crown-6)), 3.67 (23 H, crown).

^{13}C NMR (200 MHz, D_2O) δ ppm: 26.8 (2 C, $-\text{CH}_3$), 34.8 (2 C, $-\text{C}_\alpha\text{H}-$), 42.5 (br, 3 C, $-\text{C}_\beta\text{H}_2-$ and $-\text{CH}_2-$ (18-crown-6)), 53.5 (1 C, $-\text{CH}_2\text{SO}_3\text{H}$), 59.3 (1 C, $>\text{C}(\text{CH}_3)_2$), 70.7 (11 C, 18-crown-6), 178 (1 C, $>\text{C}=\text{O}$, crown), 179.2 (1 C, $>\text{C}=\text{O}$, AMPS).

Synthesis of PAMPS. PAMPS was synthesized as described by Wang et al.¹⁸ and purified by dialysis. The polymer was dried in vacuo at room temperature; $m(\text{polymer}) = 21.9$ g, yield 73%. The $\text{p}K_a$ value of PAMPS is 1.16 ± 0.05 , which is determined by potentiometric titration of 0.1 M PAMPS solution at 1.0 M NaCl with 0.1 M NaOH solution.

M_n (SEC, PAA standards) = 152 000 g/mol, PDI = 2.31. A PAMPS chain with molecular weight of M_n has a contour length of 186 nm.

^1H NMR (200 MHz, D_2O) δ ppm: 1.54 (8 H, $-\text{CH}_3$ and $-\text{C}_\beta\text{H}_2-$), 2.16 (1 H, $-\text{C}_\alpha\text{H}-$), 3.04, 3.38 (2 H, $-\text{CH}_2-$).

Selection of Substrate. Polyelectrolytes behave differently on different substrates, which make the selection of proper substrate important. The polyanion (the polymers used in this study) prefers to adsorb onto positively charged surface from aqueous solution, such as amino-modified quartz. If we select propylamine ($\text{p}K_b = 3.4$) as analogue, the amino groups would be ionized almost totally when $\text{pH} < 8.6$. Since in water, the generally homogeneous surface of amino-modified quartz may facilitate a uniform adsorption conformation for the polymer adsorbates, which will result in a smooth desorption upon peeling off. Thus, we choose amino-modified quartz as the substrate for the study of single chain desorption. The analysis of single chain rigidity needs a strong adhesion of discrete segments to the surface.¹⁵ The cover glass has a multicomponent surface, which may facilitate a strong adhesion of discrete polymer segments on it. Usually, the strong adhesion anchor points can bear a stretching force up to a few nanonewtons (nN), which enables the analysis of single chain rigidity. Therefore, we select cover glass as the substrate for the study of single chain rigidity.

Substrates Preparation. Two kinds of slides were used as substrates. Cover glass: The cover glass was cleaned by hot "piranha" solution (7:3 98% H_2SO_4 /35% H_2O_2) and followed by extensive rinse with DI water before use. Amino groups modified quartz slide: The hydroxylated quartz slide pretreated by hot "piranha" solution was immersed into a toluene solution of 3-aminopropyltrimethoxysilane (v/v = 1:1000) and kept in the solution for about 8 h. Prior to use, it was rinsed with toluene and chloroform, respectively, and dried in air. The aminosilane coverage of the substrate is $\sim 95\%$, which has been studied in our previous study by X-ray photoelectron spectroscopy.¹⁶

Sample Preparation. The slide prepared in the way as mentioned above was immersed in the aqueous PAMPS or PAMPS-co-crown solution (10 mg/L) for 5 min. After that, the slide was rinsed with DI water to remove the loosely adsorbed molecules. This would result in an ultrathin polymer film on the substrate.¹⁹ After dried by air flow, the slide was mounted onto the SMFS setup for the force measurement.

Force Measurement. All force experiments were carried on a homemade AFM equipment.^{3,20} Commercial silicon nitride V-shaped cantilevers from Park Inc. (Park, Sunnyvale, CA) were used. The spring constants of the cantilevers were calibrated by measuring their thermal excitation,²¹ and the values were in the range 0.02–0.04 N/m. The stretching velocity (retraction speed of the piezo tube) varied from 60 to 2720 nm/s. The experimental details of SMFS have been described elsewhere.^{3,20} Prior to the measurements, a drop of liquid, acting as the buffer solution, was injected between the substrate and the cantilever holder, and then both the substrate and the cantilever were immersed in the buffer. In this work, we utilize three kinds of good solvents of the polymers as buffer: (1) DI water, (2) 0.1 M KCl aqueous solution, and (3) 0.9 M KCl aqueous solution. The pH values

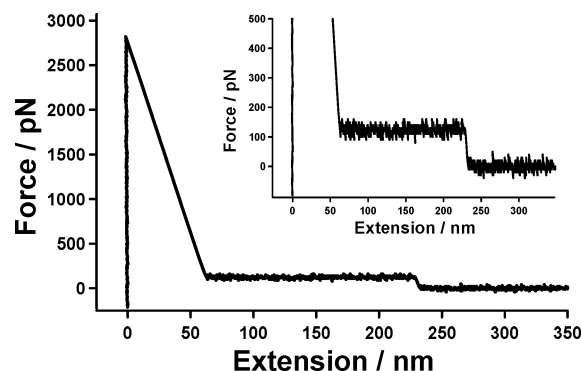


Figure 1. Typical force curve of PAMPS that shows a long plateau with height of ~ 120 pN. The buffer is DI water.

of all the buffers are in the range 5.7–6.7. By the movement of the piezo tube, the sample was brought to contact with the AFM tip for ca. 1 s under a contact force of several nanonewtons, and the polymer chains would physisorb onto the tip, producing a connective bridge in between. During the separation of the tip and the sample, the polymer chain was stretched and the cantilever would deflect. At the same time, a deflection–extension curve was recorded and then converted into a force–extension curve (in brief, force curve).³ In this study, each result is based on several parallel experiments that different samples and AFM tips were used.

It has been shown that the adhesion force between AFM tip and polymer chain can hold even to the magnitude of nanonewtons,^{3,13,20} which makes it possible for us to measure the weak intermolecular interactions between the polymer chain as well as the elasticity of the single polymer chain.

Results and Discussion

Desorption of Single Polymer Chain from Oppositely Charged Surface. Figure 1 shows the typical force curve of PAMPS obtained from amino-modified quartz in the buffer of DI water. The sharp peak in the initial stage of each force curve corresponds to the strong adhesion force between the bare tip and the uncovered regions of the substrate.³ The tip has a curvature of 20–50 nm at its apex. Comparing the cross section of an extended polymer chain (< 1 nm), the tip is much larger. For the case that one polymer chain is captured by the tip, only little of the apex surface area is affected, and the strong interaction between the tip and substrate is retained. Subsequently followed by a long plateau, then the force drops to zero, indicating a rupture of the polymer bridge. The distance from the initial stage to the end of plateau is about 230 nm, giving an apparent contour length of the polymer chain being stretched. Since the polymer sample is polydisperse, the apparent contour length can be longer than the contour length calculated with M_n . The applied force keeps constant in the whole range of plateau, which indicates that no elastic elongation occurs on the polymer chain being stretched. Because of the repulsion between monomers, the strongly charged polyelectrolyte chain assumes an extended conformation in solution,²² which facilitates an adsorption of single chains in a trainlike conformation on the surface with opposite charge. When the long adsorbed train is attached, the AFM tip retraction progressively unzips the sequence of its binding sites with the surface and the force should remain constant, resulting in a long plateau in the force curve.^{14,16} The desorption force of the single PAMPS chain from the substrate, indicated by the height of the long plateau, remains ~ 120 pN along the desorption (unzipping) process (see more clearly from the inset of Figure 1).

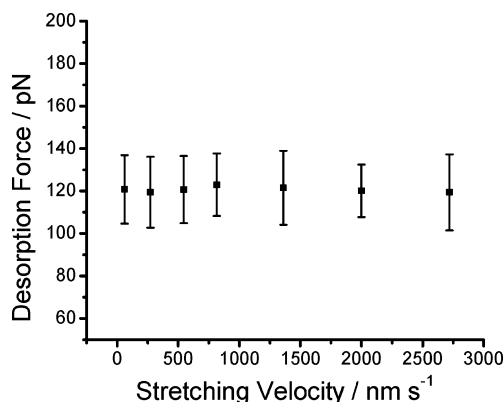


Figure 2. Desorption force of PAMPS as a function of the stretching velocity of the SMFS equipment. The standard deviation (error bar) of each point was calculated on the basis of thousands of data points from tens of force curves; see also Figure 3.

The rather low desorption force does not allow us to realize forward and backward stretching. However, we can verify whether the desorption/adsorption process is in equilibrium or not by changing the stretching velocity. We find that the desorption force is independent of the stretching velocity from 60 to 2720 nm/s (see Figure 2). Some of the statistical histograms of the desorption force at given stretching velocity are presented in Figure 3, from which we can see that the standard deviation of the desorption force are close to the noise level. The narrow distribution of the desorption force supports that the results are obtained from single chain manipulation.

Soft polymer linkage usually introduces complicated deviations in bond strength under steady speed detachment, which made the calculation of loading rate ($\Delta\text{force}/\Delta\text{time}$) difficult.²³ In our case, the PAMPS chain was smoothly peeled off from the surface without further elastic extension or yield. We can therefore conclude that the each unit of the stretched strand is moving synchronously with the AFM tip along the desorption process without damping or elongation. That is to say, here we can calculate the loading rate of our desorption experiment easily, even if it is a polymer chain being stretched. In the range 2.28–116.1 nN/s, the desorption force is loading rate independent, as shown in Figure 4. It has been elucidated that an enhanced external force is required to shorten the lifetime of a noncovalent bond between two molecules/structures.²³ In the present study, the loading rate independent result implies that the lifetime of the bond between the PAMPS chain and the substrate is much shorter than the time scale in our experiments (0.1–1 ms), and the desorption process is carried out in an equilibrium state.^{3,23,24} Thus, the adhesion force between PAMPS chain and the substrate is equal to the desorption force obtained. Although we find an independence of the desorption force on the loading rate in our system, it could be possible to discover the pronounced variation of the desorption force at the nonequilibrium state in ultrahigh loading rate region in the future, which will fill in the gap between the theory and experiment.²³

To replace water by the solution of inorganic salt, we have studied the effect of electrolyte on the desorption force of PAMPS from the amino-modified quartz. We did not find evident change after introducing high concentration of KCl (0.9 M); i.e., the long plateaus obtained still have the constant height of ~ 120 pN. From intuition, this result is inexplicable since the interaction

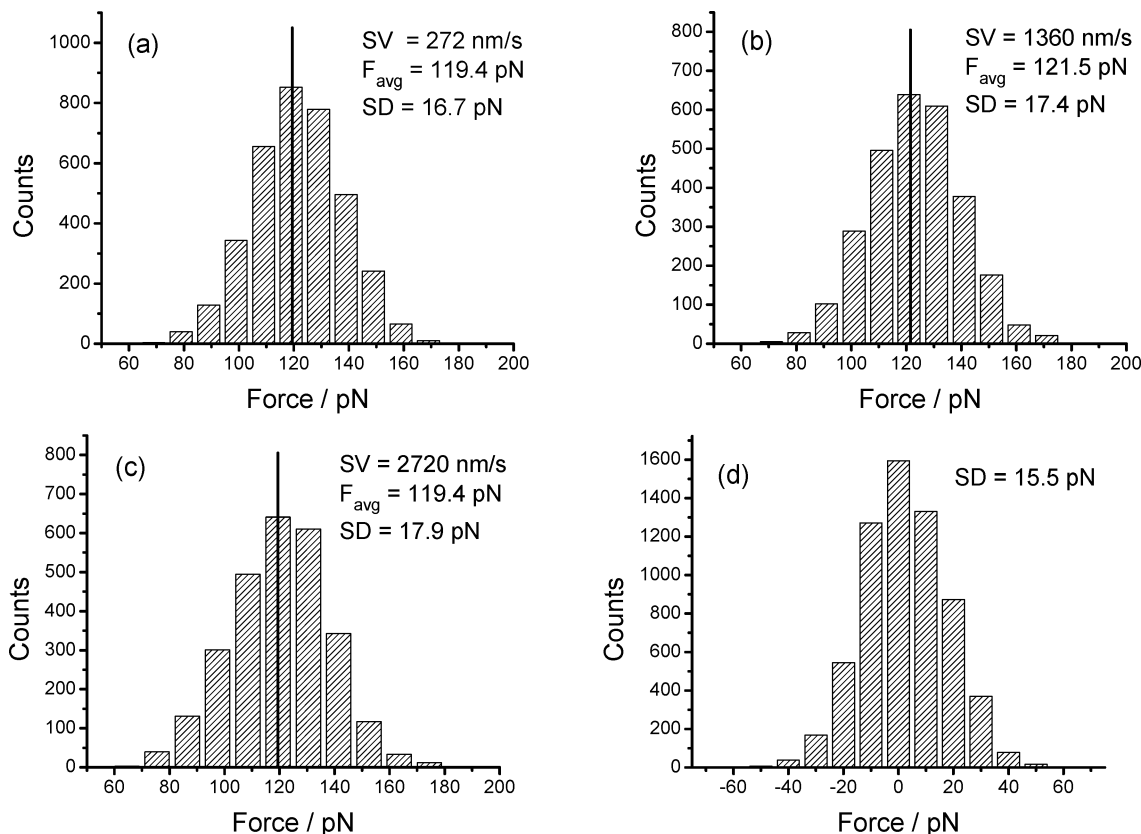


Figure 3. Statistical histograms of the desorption force of PAMPS obtained in DI water at given stretching velocity: (a) 272, (b) 1360, and (c) 2720 nm/s. The average desorption force (F_{avg}) and the standard deviation (SD) of each condition are provided. For comparison, the noise of the blank curve obtained at 272 nm/s is also analyzed, as shown in (d).

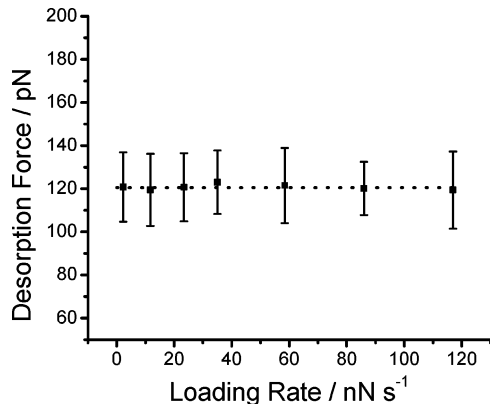


Figure 4. Desorption force of PAMPS as a function of the loading rate.

between the polyelectrolyte and substrate should be screened by the external salt in some extent. To find the possible explanation, we tried to introduce a lower salt concentration, 0.1 M KCl, into the sample that long plateaus had been obtained frequently under DI water just a few seconds before. This time, we found that it was difficult to catch polymer chains. It seems that most polymer chains were diffused into the buffer solution since the external salt would screen the electrostatic attraction between the polyelectrolyte chains and the substrate. In this situation, the polyelectrolyte chains would prefer to be dissolved into the buffer solution. Thus, the probability for the AFM tip to catch polymer chains from the solid support is reduced dramatically, as observed in our experiments. Even so, we still obtained long plateaus for the PAMPS sample in the 0.1 M KCl buffer with a lower probability ($\sim 1/50$, while

in DI water, $\sim 1/5$), which also showed a desorption force at ~ 120 pN. These series experiments show that the external salt does not influence the desorption force and the adsorption conformation of PAMPS but only the adsorption amount of the polyelectrolyte. The amino groups bearing on the substrate have two forms: the charged ammonium groups and the uncharged amino groups. The hydrophobic nature of the substrate (the static contact angle is $\sim 67^\circ$) implies that there exist considerable uncharged amino groups. The PAMPS chain also has two facets: a hydrophobic backbone and the charged side groups (see Scheme 1 for the primary structure of the polymer). The spacer between backbone and charged group combines the two features in one polymer chain but does not erase any of them. Hence, PAMPS can adsorb onto either the hydrophobic uncharged or hydrophilic charged area of the substrate via hydrophobic interaction (the effective attractions between apolar groups in water) or electrostatic interaction, respectively. It is helpful to note that other researchers also found that polyelectrolyte with spacers prefer to adsorb onto the hydrophobic regions rather than hydrophilic area.²⁵ In our experiments, when the sample is immersed in the salt solution, the ion screening effect would influence largely on the electrostatic interaction but little on the hydrophobic interaction between PAMPS and substrate. As a result, the adsorption amount of PAMPS decreased remarkably, as indicated by the lower probability for capturing PAMPS chains in the experiments. The unchanged desorption force obtained in varying salt concentration is rationalized as follows: the adhesion/desorption force is a time average result of the interaction between the polymer and the substrate. The amino groups on the substrate

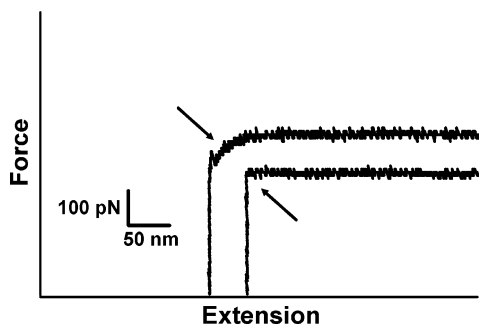


Figure 5. Typical approaching force curves obtained in different buffers from the PAMPS sample. The upper force curve is obtained in DI water. There is an evident repulsion force before the contact point, as pointed by the arrow. The lower force curve is obtained in 0.9 M KCl. No evident repulsion force is observed before the contact point.

shift between their two forms (amino and ammonium) quickly in a dynamic way.²⁶ As discussed above, PAMPS can interact with both the two forms of amino groups. Since the kinetics rate of the amino shift is far beyond the loading rate we can apply in the experiments, the desorption force measured is a time average value, i.e., an equilibrium value. Therefore, when the electrostatic interaction is screened, the hydrophobic interaction stabilizes the adhesion force between the still adsorbed PAMPS chains and the substrate. In this way, we obtained the same desorption force independent of salt concentrations. It is reported that there was a “zero charge contribution” by ~ 38 pN in the ionic strength sensitive desorption force even for the polyelectrolyte without spacer.¹⁷ In our case, the introduced spacer between the charged group and the backbone effectively enhanced the nonelectrostatic contribution to the interfacial interaction, making the interfacial interaction insensitive to the ionic strength. These two results together revealed the nonelectrostatic origin for the adsorption of the polyelectrolytes.

One may argue that the long plateau obtained could also be attributed to the behavior of Rayleigh instability of a polymer globule.²⁷ However, the buffers used in the present study are all good solvents for PAMPS and PAMPS-*co*-crown. Since the Rayleigh instability occurs only in poor solvent, we believe that the long plateaus correspond to the desorption process of a single polymer chain from the substrate, even in a high salt concentration.

A polyelectrolytes bearing surface can develop an electric double layer in aqueous solution. In the present study, we found that the double-layer force can be observed in the approaching force curve (see Figure 5). For the cases that the retracting force curves present a long plateau resembling that shown in Figure 1, the corresponding approaching force curves differ in different buffer solution. In DI water, the double-layer force (repulsion force) is clearly observed before the contact point, whereas in 0.9 M KCl it disappears. In a solution with high ionic strength, the diffuse layer is compressed remarkably since there are enough counterions in the Stern layer. On one hand, the absence of the repulsion force before the contact point reflects the high salt concentration. On the other hand, it indicates that the Stern layer is too thin to be detected by the AFM. This result supports our hypothesis that the polymer chain adopts a flat conformation on the substrate surface even in high salt concentration, which would yield minimal

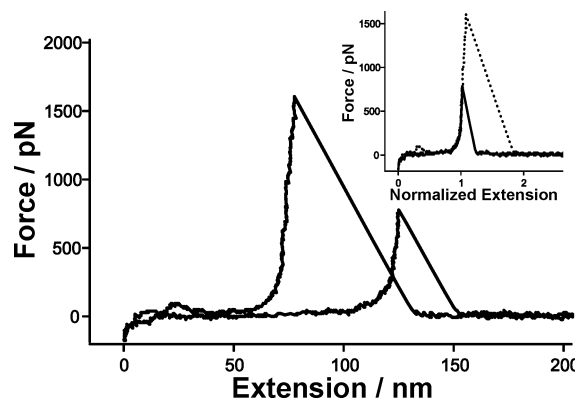


Figure 6. Typical force curves of PAMPS obtained on cover glass in DI water. Inset: the normalized force curves can be superimposed well.

steric forces. Otherwise, the Stern layer will be detectable.

Similarly, the desorption of PAMPS-*co*-crown from amino groups modified substrate was studied in the buffer of DI water. The typical force curves obtained in this case resemble that shown in Figure 1. This finding indicates that PAMPS-*co*-crown chains also assume a trainlike conformation at the interface. Furthermore, we find that the desorption force of PAMPS-*co*-crown, also independent of the loading rate, is equal to that of PAMPS. The ammonium ion bearing on the substrate can form complex with 18-crown-6.²⁸ However, our result indicates that the 20% content of crown ether side groups in the copolymer chain did not influence the desorption force. We speculate that the crown ether side groups do not interact with the amino/ammonium groups on the substrate. Potassium ion can form complex with 18-crown-6. It is of interest to observe the effect of the potassium ion on the desorption force of PAMPS-*co*-crown. Nevertheless, the desorption force as well as the force curve shape of PAMPS-*co*-crown obtained in the buffer of 0.1 and 0.9 M KCl is the same as that obtained in DI water. In the buffer containing high concentration of K^+ , almost all crown ether groups should form complex with potassium ions. The positively charged complex is repulsive to the substrate with the same charge. The invariable desorption force in the condition with or without KCl confirms our presumption that the crown ether side groups do not contribute to the adsorption/desorption force. In other words, the interaction between PAMPS-*co*-crown chain and the substrate is mainly dominated by the hydrophobic interaction.

Single Chain Rigidity of the Homopolymer and Copolymer. The behavior of single polymer chain at high forces is beyond entropic elasticity.³ We prefer to use the term “rigidity” instead of “elasticity” to express the elongation behavior of single polymer chain at high force region. The rigidity of single polymer chain is affected by many factors, such as side substitutes,^{13,29} the interaction between the solvent and the polymer chain,²⁰ and the salt concentration of the buffer solution.^{17,30} The homopolymer (PAMPS) and the relative copolymer (PAMPS-*co*-crown) are good examples to study the effect of linear charge density on the rigidity of single polymer chain. Figure 6 shows the typical force curves of PAMPS obtained from cover glass in DI water. The force rises monotonically with extension, corresponding to the increasing restoring force during the elastic elongation. Then the force drops rapidly to zero,

reflecting the rupture of the polymer bridge. Because of both the polydisperse nature of the polymer and the uncontrolled stretching point of an AFM tip, the apparent contour lengths of PAMPS vary, as shown in Figure 6. To compare the force curves of the polymer for different contour lengths, the force curves were normalized by their extension corresponding to a same force (e.g., 500 pN). The superimposition of normalized force curves (see the inset of Figure 6) indicates that the rigidity of the polymer scales linearly with its relative extension, and the force curves present the single chain rigidity (elasticity) of PAMPS.^{11,13,29}

It is well-known that the modified freely joint-chain (M-FJC) model and modified wormlike-chain (M-WLC) model can present the rigidity (elasticity) of many single polymer chains semiquantitatively though they are only a simple approximation.^{3,4} The M-FJC model, which is based on the Langevin function,^{20,31} treats a macromolecule as a chain of statistically independent segments. It is helpful to note that the Langevin function itself (FJC model) is based on rigorous statistical mechanics, but the modification should be viewed as an empirical model. The end–end distance can be calculated by the function of M-FJC model:

$$R(F) = \{ \coth[(F l_k)/(k_B T)] - (k_B T)/(F l_k) \} (L + n F / K_{\text{segment}}) \quad (1)$$

Here, F is the external force applied upon an individual polymer chain, R represents the extension of polymer chain (end–end distance), L is the contour length of the polymer chain, n is the number of segments being stretched and can be given by L/l_k , k_B is the Boltzmann constant, and T is temperature. The deformation of segments is characterized by the segment elasticity, K_{segment} . The length of the segment is Kuhn length (l_k), and the segments, which can be deformed under the stress, are freely joined together. The parameters l_k , L , and K_{segment} are allowed to vary freely. This model will provide an end–end distance (R) corresponding to a given external force (F) and a set of parameters (l_k , L , and K_{segment}). The “right” parameters will lead to a fitting force curve that can be superposed with the experimental force curve. The Kuhn length and the segment elasticity represent the elasticity/rigidity of an individual polymer chain. Since different polymers have different l_k and K_{segment} , it is hard to compare the rigidity between the two polymers. It is reported that the product of the l_k and K_{segment} can be used as the normalized segment elasticity, K_0 , which is a standard value ready for comparison.^{3,32} In this way, the M-FJC model can be rewritten as follows:

$$R(F) = \{ \coth[(F l_k)/(k_B T)] - (k_B T)/(F l_k) \} (L + L F / K_0) \quad (2)$$

In the present study, each parameter provided by the M-FJC model is based on 10–20 force curves obtained from different samples and has a narrow distribution (the standard deviation for K_{segment} and l_k is less than 10%), and the following data are the average values. The narrow distribution of the fitting parameters supports that the force–extension curves result from single chain elongation. For comparison, the experimental force curves were also fitted by the M-WLC model:

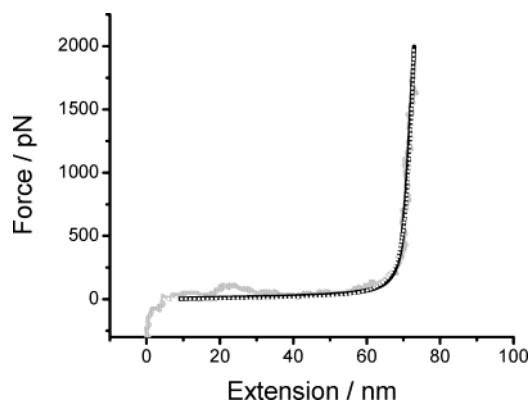


Figure 7. Theoretical models can fit the experimental force–extension curve well. The gray solid line is the experimental curve of PAMPS obtained in DI water, the black solid line is the M-FJC fitting curve ($l_k = 0.5$ nm and $K_0 = 55\,000$ pN), and the white dotted line is the M-WLC fitting curve ($l_p = 0.5$ nm and $K_0 = 2.0 \times 10^5$ pN).

$$F \frac{l_p}{k_B T} = \frac{R}{L} - \frac{F}{K_0} + \frac{1}{4(1 - R/L + F/K_0)^2} - \frac{1}{4} \quad (3)$$

The persistence length, l_p , like the Kuhn length (l_k), represents the flexibility of the polymer chain. Other parameters are similar to those involved in the M-FJC model.^{3,4}

We find that the experimental force curve can be fitted well by both the two models, as shown in Figure 7. The M-FJC fitting parameters of PAMPS in DI water, $l_k = 0.5$ nm and $K_{\text{segment}} = 1.1 \times 10^5$ pN/nm, suggested $K_0 = 55\,000$ pN, which shows that the homopolymer, PAMPS, is rather stiff.³³ This point can be supported by the M-WLC fitting parameters, $l_p = 0.5$ nm and $K_0 = 2.0 \times 10^5$ pN. This fact is understandable since PAMPS is a fully charged polymer. Each unit contains a strong electrolyte, sulfonic group. At free states, the repulsion of adjacent sulfonic groups leads to an effective stiffening of the chain.^{17,34} While upon stretching by external forces, the charges in the polymer chain can bring the coulomb repulsion and make it difficult for the torsion and rotation of the repeating units in the polymer chain upon elongation. This should be the reason for the high rigidity (elasticity) of PAMPS in DI water. Similarly, the force curves presenting the single chain rigidity of PAMPS-*co*-crown in DI water is obtained on the cover glass. The M-FJC fitting suggests that the l_k of PAMPS-*co*-crown is 1.0 nm, which is larger than that of PAMPS (0.5 nm). At the same time, the rigidity of PAMPS-*co*-crown reduced to $K_{0,\text{FJC}} = 12\,000$ pN ($K_{0,\text{WLC}} = 22\,000$ pN), which is much lower than that of PAMPS. This is reasonable since the neutral side groups of crown ether were randomly inserted into the polymer chain, which effectively reduced the linear charge density, giving rise to a lower energy barrier during elongation. As a result, the rigidity of the single polymer chain decreased remarkably.

As the concentration of counterion (K^+) increased in the buffer solution, the rigidity of PAMPS reduced remarkably (see Figure 8). In 0.1 M KCl, the normalized segment elasticity of PAMPS is $K_{0,\text{FJC}} = 11\,500$ pN ($K_{0,\text{WLC}} = 15\,000$ pN), and in 0.9 M KCl, $K_{0,\text{FJC}} = 5500$ pN ($K_{0,\text{WLC}} = 7200$ pN). These findings imply that in DI water the charges of PAMPS are screened little or even not at all. The ultrathin film of PAMPS immersed in water acts like an ultradilute polyelectrolyte aqueous

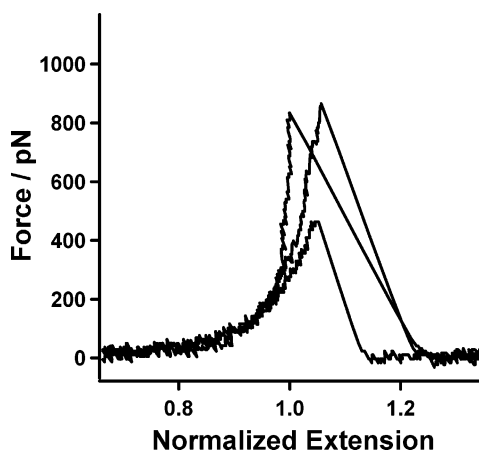


Figure 8. Normalized force–elongation curves of PAMPS show rigidity of single chain: left curve, in DI water; middle curve, in 0.1 M KCl; right curve, in 0.9 M KCl.

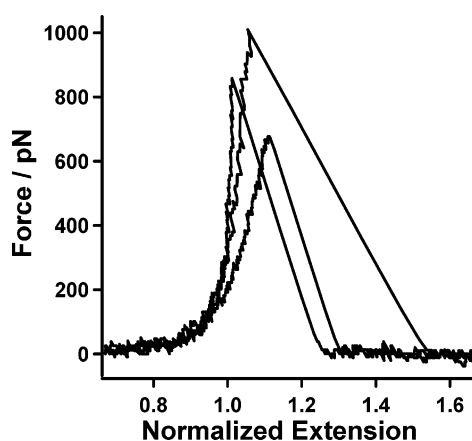


Figure 9. Normalized force–elongation curves of PAMPS-*co*-crown show rigidity of single chain: middle curve, in DI water; right curve, in 0.9 M KCl. For comparison, the force curve of PAMPS obtained in DI water is also shown (left curve).

solution. In a recent proposed model, polyelectrolytes present three phases that perform differently in a dilute solution.³⁵ For PAMPS in ultrathin film, the counterions of PAMPS are diffused into the DI water buffer. This situation is called “unsaturated condensation”; i.e., the counterions in the “cylindrical cell” are far from enough to screen the charges of PAMPS.³⁵ In the addition of external salt, the cations in the “cylindrical cell” start to take effect on the charge screening. With the charges screened, the rigid polyelectrolyte chains become flexible, indicated by the smaller K_0 , no matter what model is used.

The PAMPS-*co*-crown chains have crown ether in side groups, which can form complex with potassium ion. Beyond charge screening effect, we hope to find the influence of crown ether complexation on the single chain rigidity. In 0.1 M KCl buffer solution, the normalized segment elasticity of PAMPS-*co*-crown is $K_{0,FJC} = 10\,000$ pN ($K_{0,WLC} = 14\,000$ pN), and in 0.9 M KCl buffer, $K_{0,FJC} = 3500$ pN ($K_{0,WLC} = 6500$ pN). The rigidity of PAMPS-*co*-crown decreased gradually with the increased concentration of KCl, showing a similar result to those of PAMPS (see Figure 9). This finding indicates that the crown ether complexation affects little on the single chain rigidity. The main reasons may be the crown ethers are connected to the backbone via spacers, and the complexation affects little on the size

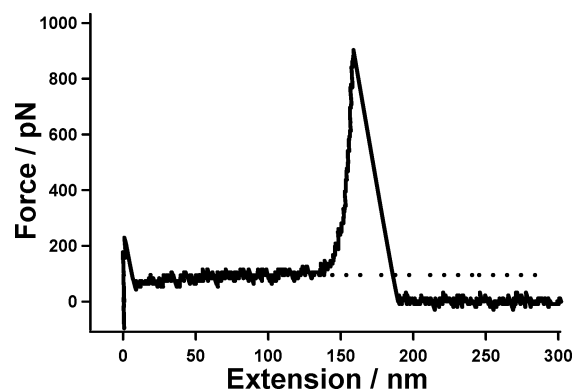


Figure 10. Special force curve of PAMPS shows two features: long plateau (smooth desorption) and peak (elastic elongation).

of the crown ether groups. The discrepancy between the single chain rigidity of the two polymers even in high salt concentration indicates that the two polymers have inherent difference, which should originate from the difference in their linear charge density.

Seamless Combination of Long Plateau and Strong Peak. In rare cases, we obtained force curves on the PAMPS/amino-modified quartz sample that have two features: a long plateau and followed by a strong peak. The long plateau has a height of ~ 120 pN, which is same to that observed previously. More interestingly, the two parts joint together seamlessly, as shown in Figure 10. This type of force curve could be achieved by the following situation: the polymer chain is adsorbed onto the substrate in a trainlike conformation, but one binding site of the chain is tightly anchored to the substrate. When the AFM tip picks up this chain from the trainlike part, the polymer chain peels off from the substrate first, which presents a long plateau in the force curve. As the desorption proceeds to the strong anchor point of the chain, the desorption process stops. However, the piezo tube does not stop at this point, and it drives the AFM tip to stretch the polymer chain further, as observed the higher and higher applied force with elongation. The M-FJC fitting result shows that this strand has a same elasticity (K_0) compared with those only present elastic-elongation peaks, as expected. The seamless joint of long plateau (smooth desorption) and strong peak (elastic elongation) in force curves, which was not reported previously, confirms our presumption that when equilibrium desorption is occurred ($F_0 k_{off}$ is much larger than the loading rate), continuous adsorption of a polymer chain leads to a long plateau and discrete adhesion leads to discrete peaks.¹⁵

Conclusions

In this paper, we have studied the effects of spacer and linear charge density on the behaviors of single polyelectrolyte chain, in terms of adhesion force and rigidity. The smooth desorption process enabled us to calculate the loading rate of the stretching process. For the two polymers, desorption forces were loading rate independent and ionic strength insensitive. Interestingly, the desorption forces of the two polymers were undistinguishable in all conditions. These findings demonstrate (1) the polymer chains adopt a trainlike (flat) conformation at the interface with a high adsorption/desorption rate, (2) the spacer, which separates the charged group from the hydrophobic backbone and combines the two properties together, should account

for the retained desorption force at high salt concentration, and (3) the 20% less in linear charge density does not affect the desorption force remarkably since hydrophobic interaction dominates the adhesion force.

In DI water, PAMPS-co-crown is less rigid than PAMPS since the uncharged side groups partially separate the charged groups, and thus the repulsion between adjacent charged groups is reduced. As the salt concentration increased, the rigidity of the two polymers both decreased, suggesting that the external salt would screen the charges of the polyelectrolytes. However, the discrepancy between the single chain rigidity of the two polymers even in high salt concentration indicates that the two polymers have inherent difference, which should originate from the difference in their linear charge density. PAMPS ultrathin film in DI water presents an "unsaturated condensation" situation, which keeps the rigidity of the single chain.

The linear charge density and the ionic strength affect only the rigidity of single polyelectrolyte chain but not the adhesion force, which is another result of the "spacer effect". This fundamental finding, which reveals the nonelectrostatic origin of the interfacial interaction of polyelectrolytes, sheds new light on the understanding of polyelectrolytes, especially for those containing spacers.

Acknowledgment. This study was supported by the Major State Basic Research Development Program (Grant G2000078102), the Ministry of Science and Technology, and the Natural Science Foundation of China (Grant 50073009). We thank Professor Hermann E. Gaub for his kindly help in establishing the SMFS setup. We also appreciate the helpful suggestions of the referees.

References and Notes

- (1) Manning, G. *J. Chem. Phys.* **1969**, *51*, 924, 3249.
- (2) Binnig, G.; Quate, C.; Gerber, C. *Phys. Rev. Lett.* **1986**, *56*, 930.
- (3) Hugel, T.; Seitz, M. *Macromol. Rapid Commun.* **2001**, *22*, 989.
- (4) Janshoff, A.; Neitzert, M.; Oberdörf, Y.; Fuchs, H. *Angew. Chem., Int. Ed.* **2000**, *39*, 3212.
- (5) Rief, M.; Gautel, M.; Oesterhelt, F.; Fernandez, J.; Gaub, H. *Science (Washington, D.C.)* **1997**, *276*, 1109.
- (6) Li, H.; Linke, W.; Oberhauser, A.; Carrion-Vazquez, M.; Kerkvliet, J.; Lu, H.; Marszalek, P.; Fernandez, J. *Nature (London)* **2002**, *418*, 998.
- (7) Smith, S.; Finzi, L.; Bustamante, C. *Science (Washington, D.C.)* **1992**, *258*, 1122.
- (8) Rief, M.; Clausen-Schaumann, H.; Gaub, H. *Nat. Struct. Biol.* **1999**, *6*, 346.
- (9) Marszalek, P.; Pang, Y.; Li, H.; Yazal, J.; Oberhauser, A.; Fernandez, J. *Proc. Natl. Acad. Sci. U.S.A.* **1999**, *96*, 7894.
- (10) Schönherr, H.; Beulen, M.; Bügler, J.; Huskens, J.; van Veggel, F.; Reinholdt, D.; Vancso, G. *J. Am. Chem. Soc.* **2000**, *122*, 4963.
- (11) Li, H.; Liu, B.; Zhang, X.; Gao, C.; Shen, J.; Zou, G. *Langmuir* **1999**, *15*, 2120.
- (12) Bemis, J.; Akhremitchev, B.; Walker, G. *Langmuir* **1999**, *15*, 2799.
- (13) Wang, C.; Shi, W.; Zhang, W.; Zhang, X.; Katsumoto, Y.; Ozaki, Y. *Nano Lett.* **2002**, *2*, 1165.
- (14) Conti, M.; Bustanji, Y.; Falini, G.; Ferruti, P.; Stefoni, S.; Samorì, B. *ChemPhysChem* **2001**, *10*, 610.
- (15) Zhang, W.; Cui, S.; Fu, Y.; Zhang, X. *J. Phys. Chem. B* **2002**, *106*, 12705.
- (16) Cui, S.; Liu, C.; Zhang, X. *Nano Lett.* **2003**, *3*, 245.
- (17) Hugel, T.; Grosholz, M.; Clausen-Schaumann, H.; Pfau, A.; Gaub, H.; Seitz, M. *Macromolecules* **2001**, *34*, 1039.
- (18) Wang, C.; Sun, Q.; Tong, Z.; Liu, X.; Zeng, F.; Wu, S. *Colloid Polym. Sci.* **2001**, *279*, 664.
- (19) Bertrand, P.; Jonas, A.; Laschewsky, A.; Legras, R. *Macromol. Rapid Commun.* **2000**, *21*, 319.
- (20) Oesterhelt, F.; Rief, M.; Gaub, H. *New J. Phys.* **1999**, *1*, 6.1.
- (21) Florin, E.; Rief, M.; Lehmann, H.; Ludwig, M.; Dornmair, C.; Moy, V.; Gaub, H. *Biosens. Bioelectron.* **1995**, *10*, 895.
- (22) Netz, R.; Joanny, J. *Macromolecules* **1999**, *32*, 9013.
- (23) Evans, E. *Annu. Rev. Biophys. Biomol. Struct.* **2001**, *30*, 105.
- (24) Evans, E. *Biophys. Chem.* **1999**, *82*, 83.
- (25) Zapotoczny, S.; Auletta, T.; de Jong, M.; Schönherr, H.; Huskens, J.; van Veggel, F.; Reinholdt, D.; Vancso, G. *Langmuir* **2002**, *18*, 6988.
- (26) Hempenius, M.; Péter, M.; Robins, N.; Kooij, S.; Vancso, G. *Langmuir* **2002**, *18*, 7629.
- (27) Bakker, H.; Nienhuys, H. *Science (Washington, D.C.)* **2002**, *297*, 587.
- (28) Luzar, A.; Chandler, D. *Phys. Rev. Lett.* **1996**, *76*, 928.
- (29) Haupt, B.; Senden, T.; Seveck, E. *Langmuir* **2002**, *18*, 2174.
- (30) Seveck, E.; Williams, D. *Phys. Rev. Lett.* **1999**, *82*, 2701.
- (31) Kado, S.; Kimura, K. *J. Am. Chem. Soc.* **2003**, *125*, 4560.
- (32) Zhang, W.; Zou, S.; Wang, C.; Zhang, X. *J. Phys. Chem. B* **2000**, *104*, 10258.
- (33) Baumann, C.; Smith, S.; Bloomfield, V.; Bustamante, C. *Proc. Natl. Acad. Sci. U.S.A.* **1997**, *94*, 6185.
- (34) Smith, S. B.; Cui, Y.; Bustamante, C. *Science (Washington, D.C.)* **1996**, *271*, 795.
- (35) Xu, Q.; Zou, S.; Zhang, W.; Zhang, X. *Macromol. Rapid Commun.* **2001**, *22*, 1163.
- (36) Compare the single chain rigidity of other polymers: the K_0 of poly(*N*-isopropylacrylamide) is 17 680 pN (ref 29), and that of poly(acrylic acid) is 8320 pN (ref 11).
- (37) Netz, R.; Orland, H. *Eur. Phys. J. B* **1999**, *8*, 81.
- (38) Deshkovski, A.; Obukhov, S.; Rubinstein, M. *Phys. Rev. Lett.* **2001**, *86*, 2341.

MA0353991